# Novel sensor technology for NDE of concrete

Xianglei Ni[a], Piervincenzo Rizzo[a1], Chiara Daraio[b]
[a]Department of Civil and Environmental Engineering, University of Pittsburgh, 3700 O'Hara Street, Pittsburgh, PA 15261;
[b]Aeronautics (GALCIT) and Applied Physics, California Institute of Technology, 1200 E California Boulevard, MC 105-50, Pasadena, CA 91125

## ABSTRACT

This paper describes the application of a novel actuator/sensor technology for the generation and detection of stress waves in structural materials like concrete. The technology is aimed at developing an innovative NDE scheme based on the generation of highly nonlinear solitary waves (HNSWs). HNSWs are stress waves that can form and travel in highly nonlinear systems (i.e. granular, layered, fibrous or porous materials) with a finite spatial dimension independent on the wave amplitude. Compared to conventional linear waves, the generation of HNSWs does not rely on the use of electronic equipment (such as an arbitrary function generator) and on the response of piezoelectric crystals or other transduction mechanism. The results of using these new actuator/sensors to test concrete slabs are presented and discussed.

**Keywords:** Highly nonlinear solitary waves, nondestructive Evaluation, novel sensors, concrete slabs.

## INTRODUCTION

The demand for inspection or monitoring of engineering structures by means of non-destructive testing (NDT) or structural health monitoring (SHM) methods is increasing rapidly. Especially, monitoring structures made of heterogeneous materials like concrete presents several challenges associated with the effectiveness of the adopted method, the capability to provide real-time information, and the possibility to deploy a sensing system permanently in the host structure. Several NDT methods to inspect concrete were proposed in the last two decades including ultrasonic testing, impact-echo, thermography, and ground penetrating radar.

Impact-echo (IE) has emerged as one of the most commonly used NDE methods for concrete defect detection since it was first proposed by researchers at the U.S. National Bureau of Standards and Cornell University [1]. The effectiveness of the IE method has been proven in a large number of civil engineering applications, including integrity testing of concrete piles [2], thickness measurement of plate-like structures, detecting delaminations in concrete slabs [3], determining the depth of surface-opening cracks [4], detection of corrosion damage of rebar in concrete [5], evaluation of grouted condition of post-tensioned bridge ducts [6], assessment of fire-caused damage of concrete [7].

IE is an NDT technique based on the propagation of stress waves. An IE testing system includes three parts: an impactor which introduces stress waves into the test specimen, a transducer (sensor) placed near the impact point that measures the motion generated by the wave propagation in the test specimen, and a data acquisition and analysis system.

The stress waves induced by the impactor onto the test specimens are longitudinal (P-wave), shear wave (S-wave), and surface (Rayleigh, R-wave) waves. The displacement of the surface close to the impact is usually dominated by the R-wave and the P-wave. Particularly, the monitored P-wave is the result of a vibrational resonance through the thickness of the element. The obtained time domain signal is transformed to frequency domain (amplitude spectrum), where the frequency value at the maximum amplitude (peak) is monitored. The dominant frequency of the P-wave is related to the thickness, $T$, and the apparent P-wave velocity for plate-like structures, $C_{pp}$ by

[1] pir3@pitt.edu ; phone 1 412 624-9575; fax 1 412 624-0135; http://www.pitt.edu/~pir3/

Sensors and Smart Structures Technologies for Civil, Mechanical, and Aerospace Systems 2009
edited by Masayoshi Tomizuka, Chung-Bang Yun, Victor Giurgiutiu, Proc. of SPIE Vol. 7292
729218 · © 2009 SPIE · CCC code: 0277-786X/09/$18 · doi: 10.1117/12.815510

$$f = \frac{\beta C_{pp}}{2T} \quad (1)$$

where $\beta$=0.96 is an empirical factor assigned to the P-wave velocity in order to correct measured $C_p$ to the apparent P-wave velocity for plates, $C_{pp}$. Recently Gibson and Popovics [8] demonstrated that the impact-echo resonance in pates is corresponding to the S1 mode Lamb wave at the zero group velocity frequency condition.

The selection of proper impactors and transducers is relevant to the success of the IE test [1], and both time and frequency domain analysis are needed to provide complementary information [9].

In this paper a novel actuator [10], based on the generation of highly nonlinear solitary waves (HNSWs), is presented. HNSWs are stress waves that can form and travel in highly nonlinear systems (i.e. granular, layered, fibrous or porous materials) with a finite spatial dimension that is independent on the wave amplitude and dependent only on the material's geometry. These waves are very stable in highly nonlinear media because when they propagate the nonlinearity of the system compensates exactly the dispersion of the wave [11]. The theoretical prediction of the stress wave propagation in a chain of identical elastic beads is given by Nesterenko [11,12] and was demonstrated through quantitative experiments [12-14]. This paper presents the preliminary results of a study where the novel actuator system is used as an impactor for an IE testing devoted to the detection of damage in a concrete slab. The data are analyzed by using conventional Fast Fourier Transform (FFT) and a joint time-frequency analysis based on the continuous wavelet transform (CWT).

## EXPERIMENT SETUP

The novel actuator is shown in Fig. 1. A PTFE tube is filled with 20 steel beads with diameter $d$=0.1875 inches. Of these 20 beads, two beads contained a lead zirconate titanate based piezogauges (PZTs), as described in [10,14]. These beads were positioned as the first and the fifteenth (from bottom to top) bead in the chain and are used to measure the amplitude and duration of waves that propagate in the chain. The actuator includes a striker made of a bead identical to the chain's beads falling from a height of 2.5 inches.

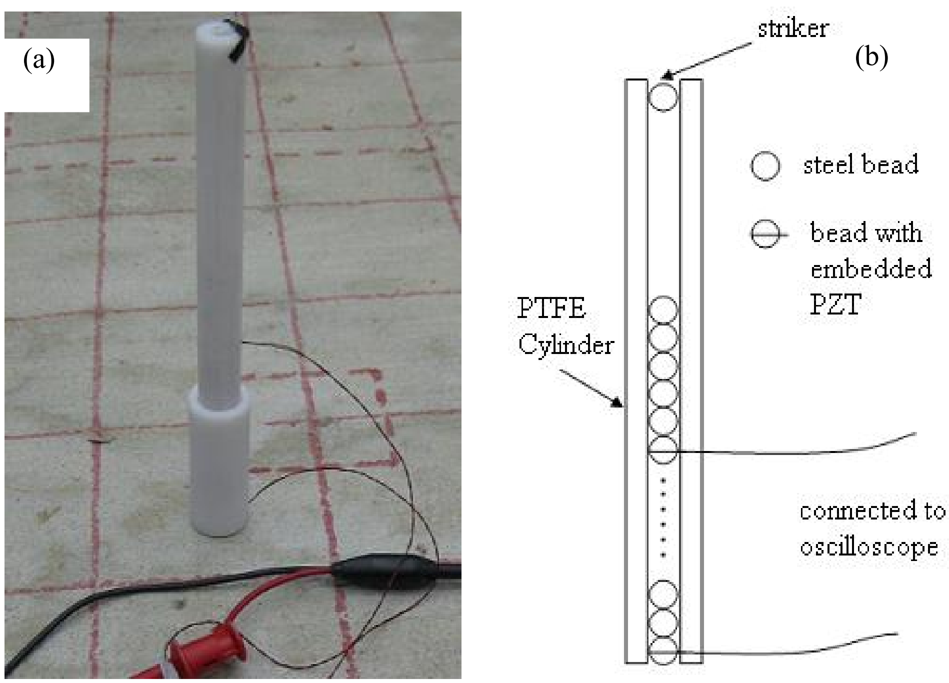


Fig. 1. (a) Photo of the highly nonlinear actuator; (b) sketch of the highly nonlinear actuator composed of a chain of identical beads.

Trains composed of a variable number of waves, with different amplitude and temporal duration, can be excited by impacting the top of the chain with strikers of different masses and velocities.

Typical pulses detected by the two PZTs are shown in Fig. 2. The pulse wave velocity $v_h$, was calculated from a travel distance 14$d$ and travel time $\Delta t$ and found to be equal to 673.5 m/s, which is one order of magnitude lower than the longitudinal wave velocity in steel (~5900 m/s)

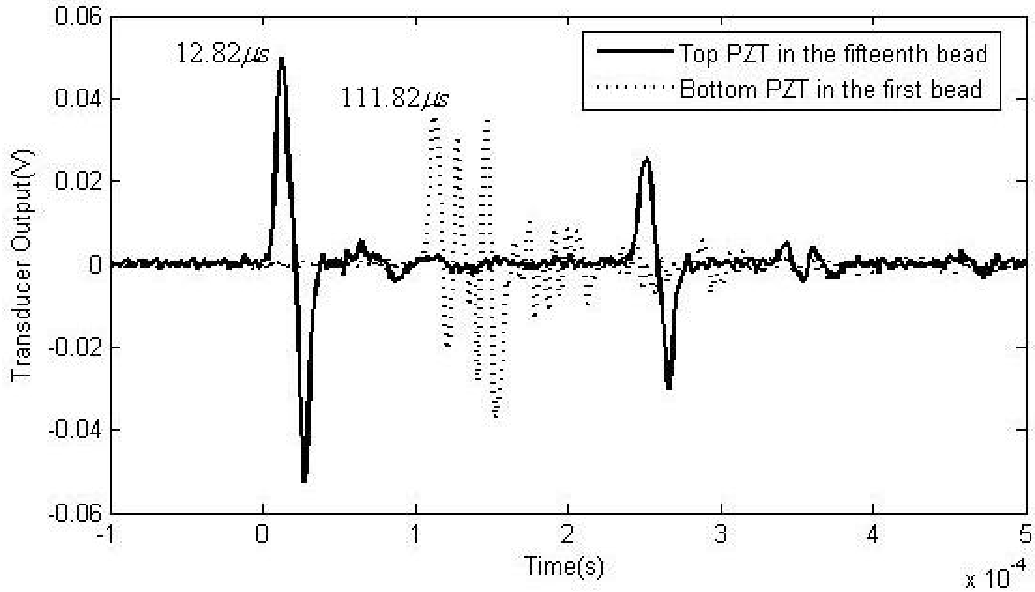


Fig. 2. Waves excited in the chain of beads

One reinforced concrete slab shown in Fig. 3 was cast for testing. The slab is 48 inches long, 36 inches wide and 6 inches thick. The slab contains 4 delaminations and 2 voids simulated by double-layer plastic sheets and foams, and it

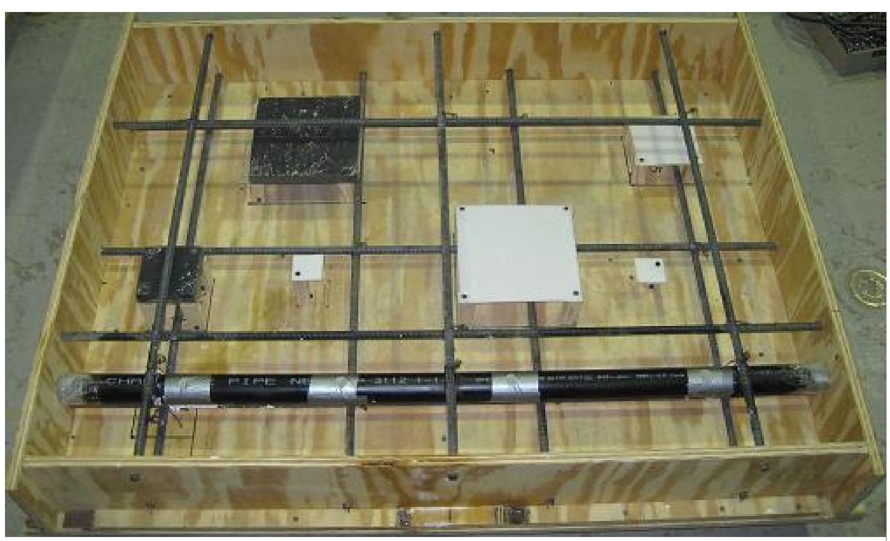

Fig. 3. Photo of the formwork of the concrete slab with defects before casting

also contains an embedded duct which is divided into 9 parts, 5 parts are voids simulated by inserted foams and other 4 parts are filled with cement pastes. The sizes and depths of the defects are measured before casting concrete and summarized in Table 1.

Table 1. Summarization of defects

| Defect number | Defect type | Defect size (inch) | Defect depth (inch) |
|---|---|---|---|
| 1 | void | 8×8 | 2.75 |
| 2 | delamination | 5×5 | 3.75 |
| 3 | void | 4×4 | 1.75 |
| 4 | delamination | 2×2 | 2.75 |
| 5 | delamination | 8×8 | 2.75 |
| 6 | delamination | 2×2 | 3.75 |

For convenience the slab was visually meshed using a grid spacing of 3 inches in both directions. Therefore 11×15=165 nodal points were identified by the grid. Such points were also the impact points where the propagation of stress waves was induced. The schematic representation of the grid and the location of the simulated defects are represented in Fig. 4. The visual imaging stage in reference [16] is followed.

The distance between the impactor and the transducer was kept equal to 3 inches everywhere except for the measurement along the pipe where the impact-sensor distance was equal to 2.4 inches. These distances corresponded to 40 to 50 percent of the thickness of the sound slab, addressing the suggested recommendation [1,3,4,16].

The transducer and the PZTs were connected to an oscilloscope and the signals were sampled at 1 MHz sampling frequency.

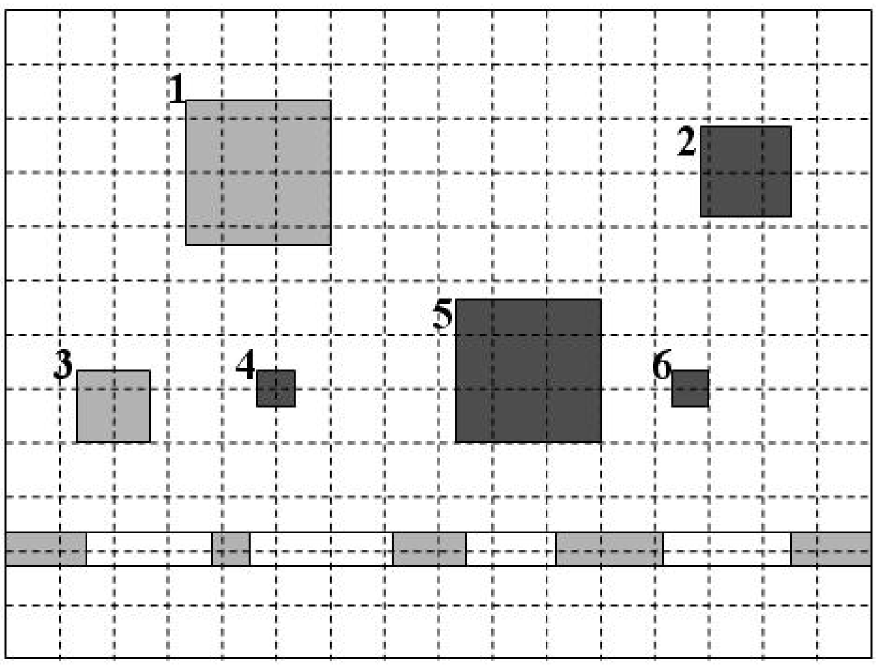


Fig. 4. Schematic plan view of the concrete slab. Light grey squares identify the simulated voids whereas the dark dark grey squares locate the simulated delaminations. The numbers identify the defect listed in Table 1.

## RESULTS AND DISCUSSION

### Data acquisition and analysis

A typical waveform measured by the transducer at points without defects is shown in Fig. 5(a). The corresponding frequency spectrum obtained by Fast Fourier Transform (FFT) is presented in Fig. 5(b). Two peaks are observed in Fig. 5(b), the one at 12.21 kHz is related to the Impact-Echo resonance. The time history and the frequency spectrum of a measured point on top of a void are shown in Fig. 5(c) and 5(d), respectively. The time history and the frequency spectrum of a measured point on top of a delamination are shown in Fig. 5(e) and 5(f), respectively. A lower frequency

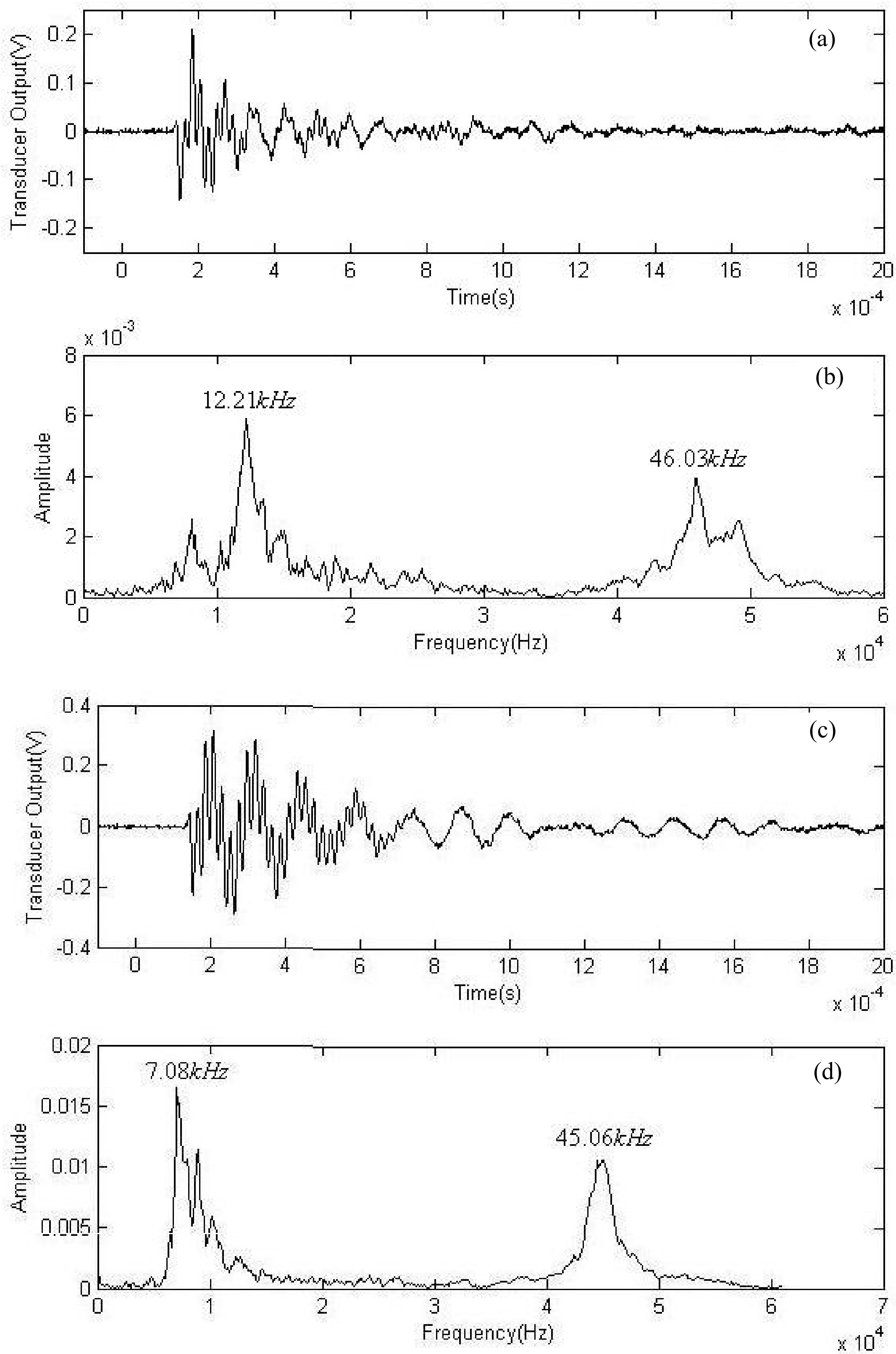
(a)
Transducer Output(V)
Time(s)
x 10^-4
(b)
x 10^-3
Amplitude
12.21kHz
46.03kHz
Frequency(Hz)
x 10^4
(c)
Transducer Output(V)
Time(s)
x 10^-4
(d)
Amplitude
7.08kHz
45.06kHz
Frequency(Hz)
x 10^4

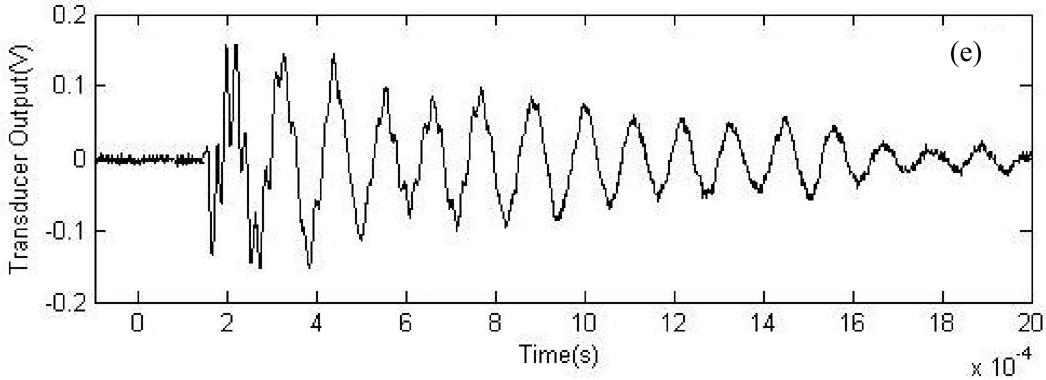


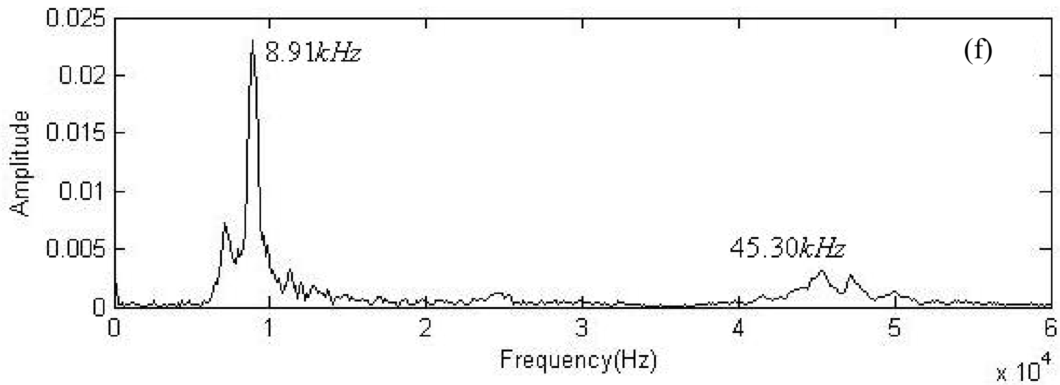


Fig. 5. (a) A typical waveform measured at points without defects. (b) The frequency spectrum of signal in (a) obtained by FFT. (c) A waveform measured at a point with void. (d) The frequency spectrum of signal in (c) obtained by FFT. (e) A waveform measured at a point with delamination. (f) The frequency spectrum of signal in (e) obtained by FFT.

peak that is related to the flexural vibration mode of the plate above the void is observed and it indicates the appearance of defects. In all cases, the presence of a higher frequency component is visible. The origin of such a component is under investigation.

**Time-frequency analysis by Wavelet Transform**

The CWT was used to calculate the time-frequency distribution of the recorded signals. The CWT relative to the time-history presented in Fig. 5(a) is shown in Fig. 6(a). The Gabor wavelet was selected as the mother wavelet. As shown in Fig. 6(b), the energy peak whose dominant frequency is between 12 to 13 kHz occurs around 192$\mu s$ and from Fig. 2, the time when the pulse passes through the bottom bead is about 112 $\mu s$, therefore, the travel time of the wave from the impact point to the sensor is 80 $\mu s$. Assuming the P-wave speed in concrete equal to 3650 mm/μs, given the thickness of the slab, the peak arrival at 80 $\mu s$ is related to the IE resonance mode.

**Visual Image**

The visual imaging method proposed in reference [16] is adopted. A 2D matrix composed of dominant frequencies (without consideration of peaks around 45 kHz) of the signals' frequency spectrums for each testing point is used to construct the visual image. All dominant frequencies of 165 testing points are stored in a 2D matrix and then plotted as a contour image in Matlab. The defects can be easily located from this contour image shown in Fig. 7.

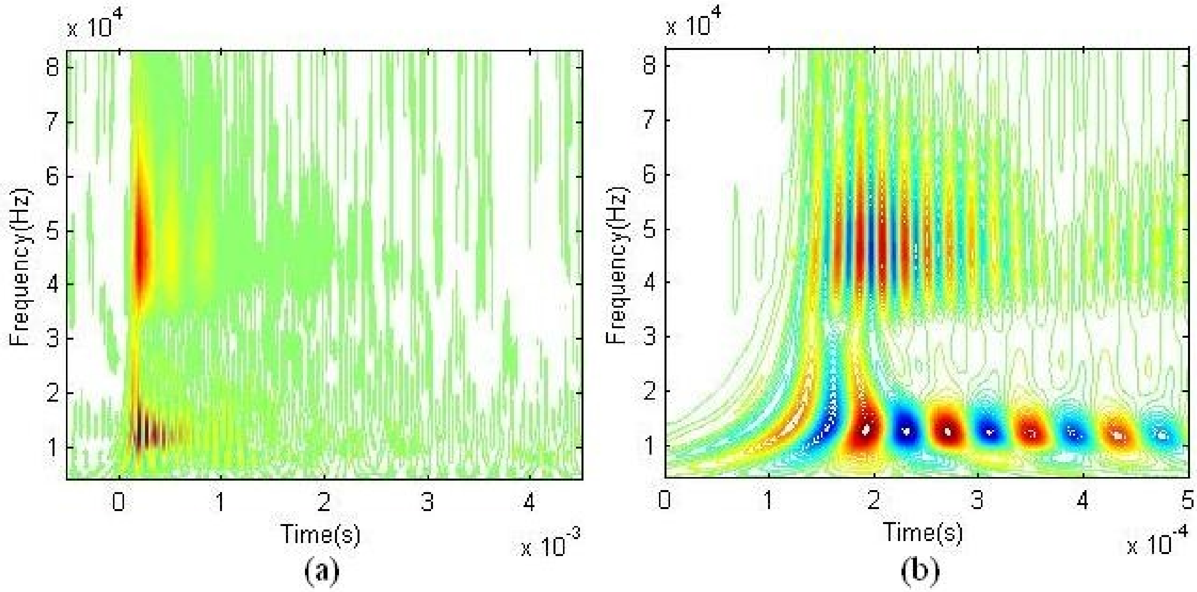


Fig. 6. The Gabor wavelet spectrum of the signal shown in Fig. 5 (a) Overall; (b) Zoom-in.

Comparing Fig. 7 to Fig. 4, it is obvious that all defects have been detected except defect 6. The dominant frequencies at defects 1, 2, 4 and 5 are lower than 12.17 kHz and they are corresponding to the flexural vibration mode. An unexpected higher frequency than 12.17 kHz is observed at the middle of the defect 3, it is considered as the influence of the intersection of two reinforcing rebars which increases the stiffness of the slab. The defect 6 has not been detected, because although the size of defect 6 is the same as that of defect 4, the depth of defect 6 is larger than that of defect 4, according to the theory in [1] the deeper the defect, the larger the minimum size of defect that can be detected. Another reason may be that there is a testing point in the center of defect 4, but there is only a testing point on the boundary of the

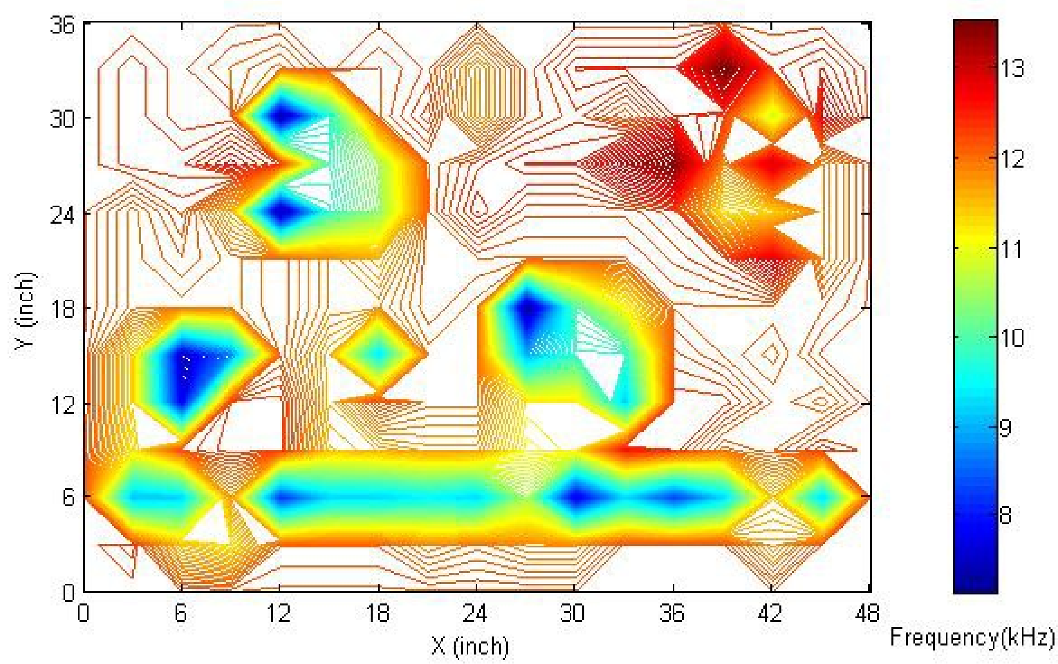


Fig. 7. 2D contour image of the concrete slab

defect 6.

All five parts of duct with bad grouted condition have been detected although the accuracy is not high. The void in the second (from left to right) sound part of the duct is detected, and it may be because the duct is not fully filled with cement paste as expected.

## CONCLUSIONS

A novel impactor based on the propagation of highly nonlinear solitary waves is presented in this paper. Its effectiveness has been demonstrated by an Impact-Echo test on a concrete slab with designed defects. Owing to its repeatability and tunability, the impactor introduced in this paper is a promising actuator/sensor for Nondestructive Evaluation and Structural Health Monitoring. Further research is required to comprehend its full potential both at a very fundamental and applied level.

The time-frequency signal processing techniques can provide information in both time and frequency domains simultaneously. More useful information can be obtained by utilizing a time-frequency analysis technique such as Wavelet Transform. Ongoing research is aimed at exploiting wavelet transform features to enhance the sensitivity of the proposed method to detect and discriminate between different types of damage.

## ACKNOWLEDGEMENTS

This work was supported by the National Science Foundation grant CMMI – 0825983 (Dr. Edoardo Misawa, Program Director).

## REFERENCES

[1] Sansalone, M.J. and Streett, W.B. Impact-Echo: Nondestructive evaluation of concrete and masonry, Bullbirer Press, Ithaca, N.Y., 1997.

[2] Steinbach, J. and Vey, E. Caisson evaluation by stress wave propagation method, Journal of the Geotechnical Engineering Division, ASCE, 1975, 101(4): 361-378.

[3] Sansalone, M. and Carino, N.J. Detecting delaminations in concrete slabs with and without overlays using the impact-echo method, ACI Material Journal, 1989, 86(2): 175-184.

[4] Sansalone, M., Lin, J. and Streett, W.B. Determining the Depth of Surface-Opening Cracks using Impact-Generated Stress Waves and Time-of-Flight Techniques, ACI Materials Journal, 1998, 95(2): 168-177.

[5] Liang, M. and Su, P. Detection of the corrosion damage of rebar in concrete using impact-echo method, Cement and Concrete Research, 2001, 31(10): 1427-1436.

[6] Tinkey, Y. and Olson, L.D. Sensitivity studies of grout defects in posttensioned bridge ducts using impact echo scanning method, Transportation Research Record, 2007, 2028: 154-162.

[7] Kumar, A et al. Impact/echo and low frequency ultrasonic testing for assessment of damage to concrete blocks exposed to sodium fire, Materials Evaluation, 2008, November, 1182-1188.

[8] Gibson, A. and Popovics, J.S. Lamb wave basis for impact-echo method analysis, Journal of Engineering Mechanics, ASCE, 2005, 131(4): 438-443.

[9] Schubert, F. and Köhler, B. Ten lectures on Impact-Echo, Journal of Nondestructive Evaluation, 2008, 27(1-3): 5-21.

[10] Eggenspieler, D. *Non destructive evaluation using phononic-crystal meta-material*, Internal report, California Institute of Technology, 2008.

[11] Nesterenko, V.F. Propagation of nonlinear compression pulses in granular media, Journal of Applied Mechanics and Technical Physics, 1984, 24(5): 733-743.

[12] Nesterenko, V.F., *Dynamics of Heterogeneous Materials*, Springer-Verlag, 2001.

[13] Coste, C., Falcon E. and Fauve S. Solitary waves in a chain of beads under Hertz contact, Physical Review E, 1997, 56(5): 6014-6117.

[14] Daraio, C. et al. Tunability of solitary wave properties in one-dimensional strongly nonlinear phononic crystals, Physical Review E, 2006, 73(2): 026610-1-026610-10.
[15] Shull, P.J. Nondestructive Evaluation: Theory, Techniques, and Applications, Marcel Dekker, New York, 2002.
[16] Zhu, J. and Popovics, J.S. Imaging concrete structures using air-coupled Impact-Echo, Journal of Engineering Mechanics, ASCE, 2007, 133(6): 628-640.
[17] Malhotra, V.M. and Carino, N.J. Handbook on nondestructive testing of concrete, second edition, CRC Press, Boca Raton, 2004.C.